Frequency Characteristics of PWM Mode Electrohydraulic Servos

By

Taizo SAWAMURA*, Hideo HANAFUSA** and Takashi INUI***

(Received January 30, 1960)

In this paper, the frequency characteristics of the PWM mode electrohydraulic servo are analyzed. A two-stage electrohydraulic servo was manufactured for experiments. A multivibrator was used for generating a rectangular pulse train and it was modified to obtain a high modulation gain of the pulse width. A spool in the servo valve moves in the waveshape of a trapezoidal pulse train. From the analysis of the spool movement, the equivalent transfer function of the PWM mode was obtained, and the frequency characteristics of the servo loop was analyzed. The various problems accompanying the PWM operation are also shown. The analytical results were verified by experiments.

1. Introduction

When an electrohydraulic servo is operated by the PWM mode, the actuator piston makes a small oscillation according to the pulse motion of a spool, and moves in response to the input signal. The dither in the actuator piston reduces the effect of the friction in the actuator and prevents the stick-slip motion, when the piston stops or moves very slowly[1]. When the input signal is large and the actuator piston moves in no small velocity, the dither is unnecessary. Therefore, it is reasonable for large error signal that the modulation of pulse width is saturated and the current to the torquemotor is not switched alternately, while for small error signal the current is in the waveshape of the rectangular pulse the width of which is modulated in proportion to the signal voltage. The rectangular pulse current to the torquemotor is generated by the multivibrator which is so modified that the modulation of the pulse width is easily saturated.

When the sinusoidal input is given to the PWM mode electrohydraulic servo, the spool moves in the waveshapes of a trapezoidal pulse train[2]. The widths of pulses are modulated in proportion to the momentary values of the sinusoidal

* Automation Research Laboratory
** Kyoto Technical University
*** Dept. of Aeronautical Engineering

input for small input amplitude. When the input amplitude becomes large, the modulation of pulse width is saturated during a part of the period of sinusoidal input.

In this paper, the spool movement is analyzed for the sinusoidal input and the equivalent transfer function is obtained. Further, the various problems accompanying the PWM operation are explained. The frequency characteristics of the servo loop are calculated by using the equivalent transfer function. Experimental results are also shown.

2. Construction of an Experimental Apparatus

The experimental appratus consits of a multivibrator, a torquemotor, a flapper-nozzle, a spool valve, an actuator and a differential transformer. The schematic diagram is shown in Fig. 1. The output of the differential transformer is used both for the feedback of the servo loop and for the record of the displacement of the actuator piston. In the PWM mode servo valve shown in Fig. 1, the movements of the flapper and the spool are restricted by the nozzles and the stoppers, respectively. The PWM mode servo valve is much simpler than the ordinary two-stage servo valve, because it is unnecessary that the spool displacement must be proportional to the error voltage in the ordinary valve. The width of the rectangular pulse generated by the multivibrator is modulated in proportion to the error voltage for small signals, while the multivibrator stops to generate pulses for large signals.

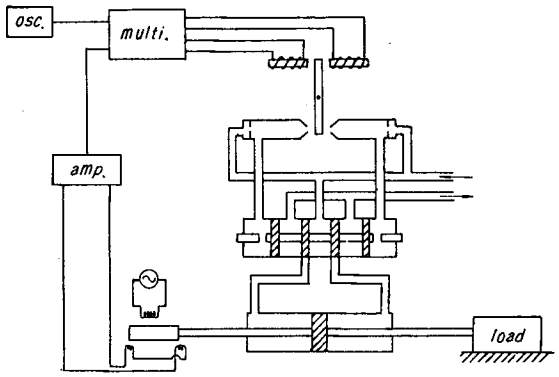

Fig. 1. Schematic diagram of experimental apparatus.

Electric current in the two coils of the torquemotor changes alternately according to the modulated rectangular pulse train, and drives the flapper. The spool is driven by a flapper-nozzle mechanism and moves in the waveshape of a trapezoidal pulse train, which lags by a constant time behind the electric current. The slope of the trapezoid depends upon the dimensions of the apparatus and the supply pressure. When the spool moves in the form of pulse train, the actuator piston oscillates in a small amplitude and moves in the direction of the input signal.

The multivibrator circuit is composed of a paraphase amplifier of 12AX7, a multivibrator of 12AU7 and a power amplifier of 6AQ5 and is shown in Fig. 2. The multivibrator is so modified that the modulation is easily saturated. As shown in Fig. 2, R_{c2} is larger and R_g is smaller than those in the ordinary circuit.

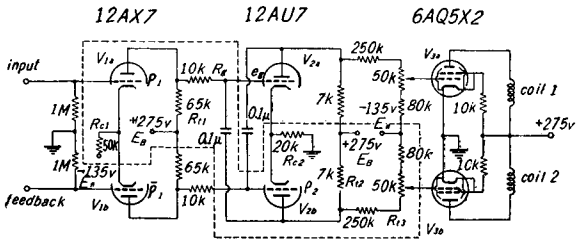

Fig. 2. Multivibrator circuit.

3. Rectangular Pulse Generated by a Multivibrator

When the plate current of V_{2a} is cut off, the equivalent circuit of Fig. 3 may be used to analyze the operation of the circuit enclosed by broken lines in Fig. 2. In Fig. 3, ρ_1 and ρ_2 are the apparent resistances of both V_{1a} and V_{2b}, respectively. It is noted that plate currents of both V_{1a} and V_{1b} flow through R_{c1}. Because 12AX7 operates as a paraphase amplifier and the constant current always flows through R_{c1}, the voltage drop is constant and is represented by E_{c1}.

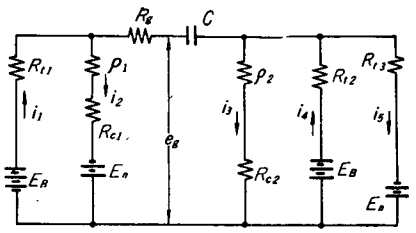

Fig. 3. Equivalent circuit of multivibrator.

By applying Kirchhoff's law to the equivalent circuit of Fig. 3, the grid voltage, e_g, of V_{2a} is obtained as follows:

$$e_g = E_B - \frac{R_{t1}}{\rho_1 + R_{t1}}(E_B + E_n - E_{c1}) - K e^{-\frac{t}{CR_e}}\left\{R_{t1} + \left(1 + \frac{R_{t1}}{\rho_1}\right)R_g\right\}, \qquad (1)$$

where K is a integral constant, and is determined by the initial value of e_g. R_e is represented as follows:

$$R_e = R_g + \frac{\rho_1 R_{t1}}{\rho_1 + R_{t1}} + \frac{R_{t2}R_{t3}(\rho_2 + R_{c2})}{(\rho_2 + R_{c2})(R_{t2} + R_{t3}) + R_{t2}R_{t3}}. \qquad (2)$$

When the plate current of V_{2a} is flowing, the grid voltage is almost equal to the cathode voltage, because the grid current flows and the voltage drop in R_g is large. At the moment that the plate current is cut off, the plate voltage of V_{2b} drops abruptly, and this voltage drop is transmitted to the grid of V_{2a}. Therefore, the initial value, e_{g0}, of the grid voltage is given as follows during the charge of the capacitor C:

$$e_{g0} = \frac{R_{c2} - R_{t2}}{R_{t2} + \rho_2 + R_{c2}} E_B. \qquad (3)$$

The integral constant in Eq. (1) is determined, substituting $e_g=e_{g0}$ and $t=0$. Replacing e_g of Eq. (1) by the cut-off grid voltage of V_{2a}, the cut-off period of V_{2a}, T_1, is obtaind as follows from Eq. (1):

$$T_1 = CR_e \log \frac{\dfrac{2R_{t2}+\rho_2}{R_{t2}+\rho_2+R_{c2}} - \dfrac{R_{t1}}{\rho_1+R_{t1}}\left(1+\dfrac{E_n}{E_B}-\dfrac{E_{c1}}{E_B}\right)}{\dfrac{R_{t2}+\rho_2}{R_{t2}+\rho_2+R_{c2}} + \dfrac{E_c}{E_B} - \dfrac{R_{t1}}{\rho_1+R_{t1}}\left(1+\dfrac{E_n}{E_B}-\dfrac{E_{c1}}{E_B}\right)}, \tag{4}$$

where E_c is the cut-off grid bias of V_{2a}. Replacing ρ_1 by the apparent resistance of V_{1b}, $\bar{\rho}_1$, in Eq. (4), the cut-off period of V_{2b}, T_1, is obtained. ρ_1 and $\bar{\rho}_1$ is changed by the grid voltages of V_{1a} and V_{1b}. If 12AX7 operates as a paraphase amplifier, the following relation is obtained.

$$\Delta\bar{\rho}_1 = \frac{(\rho_{10}+R_{t1})\Delta\rho_1}{\rho_{10}+R_{t1}+2\Delta\rho_1}, \tag{5}$$

where ρ_{10} is the apparent resistance of V_{1a} and V_{1b} for no input, and $\Delta\rho_1$ and $\Delta\bar{\rho}_1$ are the changes of ρ_1 and $\bar{\rho}_1$ from ρ_{10}, respectively. The pulse period T_0 is the sum of T_1 and $\overline{T}_1$. Using the circuit of Fig. 2, T_1, $\overline{T}_1$, T_0 and $(T_1-\overline{T}_1)/T_0$ are obtained, as shown in Fig. 4. $(T_1-\overline{T}_1)/T_0$ represents the modulation rate of the rectangular pulse width. In Fig. 4, the abscissa shows the input voltage E for the paraphase amplifier. When the input voltage becomes 0.58 volt, the alternation of plate currents of V_{2a} and V_{2b} does not occur, and the modulation rate is saturated. When the input voltage is small, the pulse period does not change, and T_1 and $\overline{T}_1$ are altered in proportion to the input voltage. When the input voltage becomes large, $\overline{T}_1$ reduces in proportion to the input as before, but T_1 increases rapidly and the pulse period becomes long. The modulation rate is proportional to the input voltage for small inputs and increases rapidly for large inputs and is saturated at last. The range in which the modulation rate is proportional to the input voltage will be called the range of linear modulation hereafter. As the effect of the pulse period is small for the equivalent transfer function of the PWM mode as will be shown after, it may be assumed that the pulse period does not change and only the modulation rate changes as shown in Fig. 4.

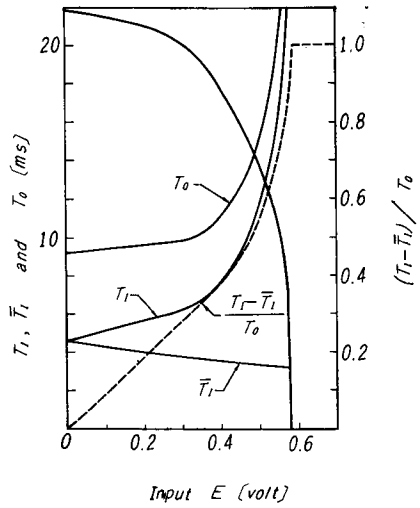

Fig. 4. Pulse periods generated by multivibrator.

Using the modulation coefficient of k, the following relation is obtained in the range of linear modulation:

$$T_1 = T_0(1+kE)/2, \tag{6}$$

$$\overline{T}_1 = T_0(1-kE)/2. \tag{7}$$

4. Motion of a Spool for DC Input Signal

When the DC input signal is given, it is assumed that the pulse period does not change and that the width of rectangular pulse is altered as mentioned above. Fig. 5 shows (i) electric current to the torquemotor, (ii) displacement of the flapper, x, (iii) displacement of the spool, y, and (iv) approximate waveshapes of the spool displacement. In Fig. 5, y_m is the clearance between the

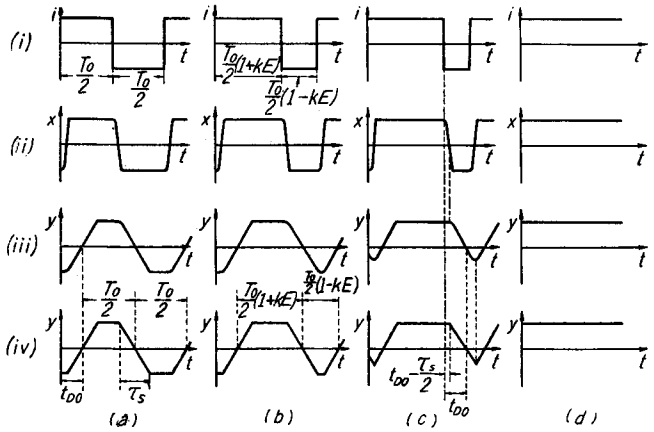

Fig. 5. Waveshapes of pulses by DC input signal.

spool and the stopper at the neutral position, t_{D0} being the time required for a spool to arrive at the neutral position after switching the torquemotor circuit, τ_s being the time length of the trapezoid slope. The waveshapes of pulses change by the input signal voltage, as shown in Fig. 5 (a), (b), (c) and (d).

(a) When the input signal is not given, positive and negative pulses are symmetrical, and the average output during one period T_0 is zero.

(b) When the input signal is small, the waveshape of the spool displacement is still trapezoidal. The average output during one period T_0 is $kEy_m T_0$ in the range of linear modulation. When the input voltage exceeds the range of linear modulation, the gain of modulation must be modified by the curve of the modulation rate shown in Fig. 4.

(c) When $k|E|$ becomes larger than $\{1-(2\tau_s/T_0)\}$, the electric current in the torquemotor is switched before the spool arrives at the stopper, and one side of

the waveshapes of the spool displacement becomes triangular. When the maximum displacement y_m is small, the multivibrator stops the generation of pulses before this state occurs.

(d) When the input voltage exceeds the saturation voltage, the output during T_0 is $y_m T_0$.

Fig. 6 shows the velocity of the actuator piston which is obtained by experiments for DC input. As the above mentioned (c) state does not exist in the experimental apparatus, the curve of Fig. 6 corresponds directly to the curve of the modulation rate of Fig. 4. The solid curve of Fig. 6 represents the connection of the experimental data. The velocity of the actuator piston is proportional to the input voltage for $E<0.25$ volt, and increases rapidly for $E>0.25$ volt. When

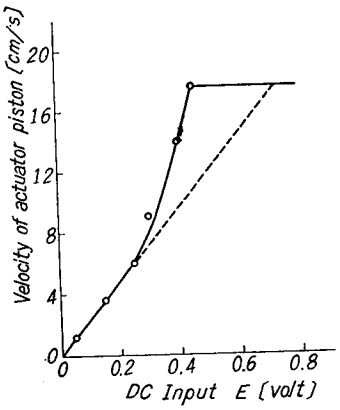

Fig. 6. Actuator piston velocity by DC input signal.

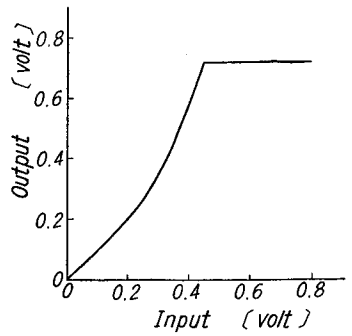

Fig. 7. Characteristics of saturation element.

$E=0.45$ volt, the dither vanishes and the modulation is saturated. The broken line of Fig. 6 shows the extension of the range of linear modulation. If the modulation gain is assumed to be constant as shown by the broken line, the input signal must be passed through an imaginary element shown by Fig. 7 before it is given to the multivibrator, so that the modulated pulse train will be the same as the actual pulse train.

5. Motion of a Spool for Small Sinusoidal Input Signal

If the origin of time is chosen at the center of the positive pulse, and the origin of the spool displacement is chosen at the base of trapezoid, the pulse train for no input signals, $e_0(t)$, is expressed by Fourier series as follows:

$$\frac{e_0(t)}{2y_m} = \frac{\tau_0-\tau_s}{T_0} + \sum_{n=1}^{\infty} \frac{1}{(n\pi)^2} \frac{T_0}{\tau_s} \sin n\omega_0\tau_s \sin \frac{n\omega_0\tau_0}{2} \cos n\omega_0 t$$
$$- \sum_{n=1}^{\infty} \frac{1}{(n\pi)^2} \frac{T_0}{\tau_s} (1-\cos n\omega_0\tau_s) \cos \frac{n\omega_0\tau_0}{2} \cos n\omega_0 t\,, \qquad (8)$$

where τ_0 is the time length of the base of trapezoid for no input signals, and ω_0 is $2\pi/T_0$.

When a sinusoidal input is given, it is assumed that the modulated rectangular pulse train has the same period as the pulse train for no input signals, and that the widths of the positive pulses are modulated symmetrically on both sides of their centers corresponding to the momentary input voltage at the centers of positive pulses. Fig. 8 shows (a) sinusoidal input, (b) electric current in the torquemotor and (c) displacement of the spool. The period of sinusoidal input is represented by T, the frequency by f, the angular frequency by ω, and the amplitude by E_a. The spool displacement lags by a constant time t_{D0} behind the electric current, and the width of the positive pulse is modulated symmetrically on both sides of its center. The modulated pulse train has the period T_a, the least common multiple of T and T_0.

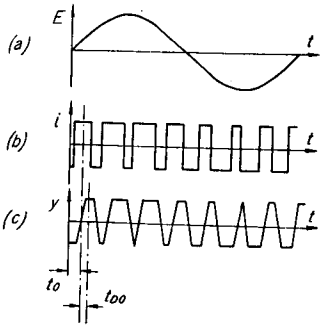

Fig. 8. Pulse trains by sinusoidal input.

As shown in Fig. 8, the origin of time is chosen at the center of arbitrary trapezoidal pulse which lags by (t_0+t_{D0}) behind the sinusoidal input. The base length τ of the m'th pulse from the time origin is given as follows:

$$\tau = \tau_0\{1+\kappa E_a \sin\omega(m T_0+t_0-t_{D0})\}, \tag{9}$$

where

$$\kappa = \frac{k}{1+(2\tau_s/T_0)}. \tag{10}$$

During the period T_a, there is only one pulse the base of which is given by Eq. (9). As the same pulse is repeated with the period T_a, this pulse train $e_m(t)$ can be written as follows, replacing τ_0, T_0 and ω_0 by τ, T_a and $\omega_a(=2\pi/T_a)$ in Eq. (8):

$$\begin{aligned}\frac{e_m(t)}{2y_m} = {} & \frac{1}{T_a}\left[\tau_0\{1+\kappa E_a \sin\omega(m T_0+t_0-t_{D0})\}-\tau_s\right] \\ & + \sum_{n=1}^{\infty}\frac{1}{(n\pi)^2}\frac{T_a}{\tau_s}\sin n\omega_a\tau_s \sin\left[\frac{1}{2}n\omega_a\tau_0\{1+\kappa E_a \sin\omega(m T_0+t_0-t_{D0})\}\right] \\ & \qquad \times\cos n\omega_a(t-m T_0) \\ & - \sum_{n=1}^{\infty}\frac{1}{(n\pi)^2}\frac{T_a}{\tau_s}(1-\cos n\omega_a\tau_s)\cos\left[\frac{1}{2}n\omega_a\tau_0\{1+\kappa E_a \sin\omega(m T_0+t_0-t_{D0})\}\right] \\ & \qquad \times\cos n\omega_a(t-m T_0). \end{aligned} \tag{11}$$

Summing $e_m(t)$ during the period T_a, the modulated pulse train $e(t)$ shown in Fig. 8 is obtained as follows:

$$e(t) = \sum_{m=0}^{f_0 T_a - 1} e_m(t)\,, \tag{12}$$

where $f_0 = 1/T_0$ is the pulse repetition rate. Substituting Eq. (11) in Eq. (12), using the relation of $\tau_0 = (T_0/2) + \tau_s$ and shifting the origin of y coordinate up to the center of the pulse height, Eq. (12) is transformed as follows:

$$\begin{aligned}
e(t) = {} & \sum_{\nu=1\,(\text{odd})}^{\infty} \frac{4y_m}{(\nu\omega\pi/\omega_0)^2} \frac{T_0}{\tau_s} \cos\left(\frac{\nu\omega T_0}{4}\right) \sin\left(\frac{\nu\omega\tau_s}{2}\right) J_\nu\left(\frac{\nu\omega T_0 k E_a}{4}\right) \sin\nu\omega(t + t_0 - t_{D0}) \\
& + \sum_{\nu=2\,(\text{even})}^{\infty} \frac{4y_m}{(\nu\omega\pi/\omega_0)^2} \frac{T_0}{\tau_s} \sin\left(\frac{\nu\omega T_0}{4}\right) \sin\left(\frac{\nu\omega\tau_s}{2}\right) J_\nu\left(\frac{\nu\omega T_0 k E_a}{4}\right) \cos\nu\omega(t + t_0 - t_{D0}) \\
& + \sum_{n=1}^{\infty} \sum_{\nu=-\infty\,(\text{odd})}^{\infty} \frac{4y_m}{(n + \nu\omega/\omega_0)^2\pi^2} \frac{T_0}{\tau_s} \cos\left\{\frac{(n\omega_0 + \nu\omega) T_0}{4}\right\} \sin\left\{\frac{(n\omega_0 + \nu\omega)\tau_s}{2}\right\} \\
& \times J_\nu\left[\frac{(n\omega_0 + \nu\omega) T_0 k E_a}{4}\right] \sin\left\{(n\omega_0 + \nu\omega) t + \nu\omega(t_0 - t_{D0})\right\} \\
& + \sum_{n=1}^{\infty} \sum_{\nu=-\infty\,(\text{even})}^{\infty} \frac{4y_m}{(n + \nu\omega/\omega_0)^2\pi^2} \frac{T_0}{\tau_s} \sin\left\{\frac{(n\omega_0 + \nu\omega) T_0}{4}\right\} \sin\left\{\frac{(n\omega_0 + \nu\omega)\tau_s}{2}\right\} \\
& \times J_\nu\left[\frac{(n\omega_0 + \nu\omega) T_0 k E_a}{4}\right] \cos\left\{(n\omega_0 + \nu\omega) t + \nu\omega(t - t_{D0})\right\}
\end{aligned} \tag{13}$$

The first and second terms on the right side of Eq. (13) represent the fundamental component and higher harmonics corresponding to the input signal. The third and 4th terms represent the output component of the pulse repetition rate and its side band component. When $T_0/T = 0.1$, $\tau_s/T_0 = 0.1$ and $kE_a = 0.6$, the frequency spectrum is shown in Fig. 9, where f is the input signal frequency, and $f_0 = 10f$ is the pulse repetition rate. As the amplitude of higher harmonics and the side band are very small as shown in Fig. 9, it is sufficient in designing the servo loop to consider only components of the input frequency and the pulse repetition rate. The output component of the pulse repetition rate should be so chosen as to cause proper dither after filtered by the low pass characteristics of the actuator.

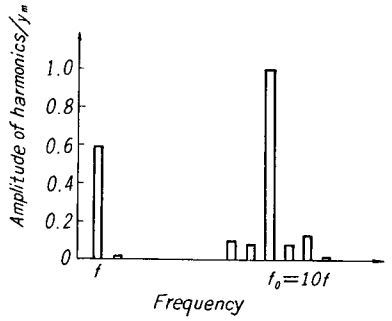

Fig. 9. Frequency spectrum of pulse train.

Considering the fundamental component of Eq. (13) exclusively, the equivalent transfer function $G_d(j\omega)$ is obtained as follows:

$$G_d(j\omega) = \frac{y_m}{E_a} \frac{16}{(\omega T_0)^2} \frac{T_0}{\tau_s} \cos\left(\frac{\omega T_0}{4}\right) \sin\left(\frac{\omega T_0}{2} \frac{\tau_s}{T_0}\right) J_1\left(\frac{k E_a \omega T_0}{4}\right) e^{-j\omega t_{D0}}\,, \tag{14}$$

where J_1 represents Bessel function. Eq. (14) holds when the amplitude of the

sinusoidal input does not exceed the range of linear modulation and the following relation is satisfied:

$$kE_a \leqq 1-(2\tau_s/T_0)\,. \tag{15}$$

When the spool displacement may be considered rectangular, τ_s reduces to zero, and the equivalent transfer function becomes as follows:

$$G_d(j\omega) = \frac{y_m}{E_a}\frac{8}{\omega T_0}\cos\left(\frac{\omega T_0}{4}\right)J_1\left(\frac{kE_a\omega T_0}{4}\right)e^{-j\omega t_{D0}}\,. \tag{16}$$

The gain of equivalent transfer function is shown in Fig. 10 for various values of T_0/T, τ_s/T_0 and kE_a. The effect of τ_s/T_0 is very small. It can be concluded that the fundamental component of the output lags by a constant time t_{D0} behind the input signal, and the effects of T_0/T, τ_s/T_0 and kE_a on the gain are very small in practice, i.e., $T_0/T<0.2$.

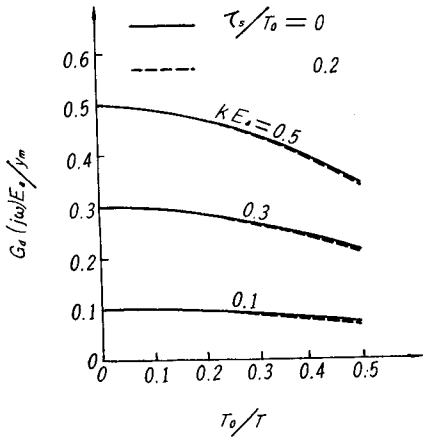

Fig. 10. Gain of equivalent transfer function.

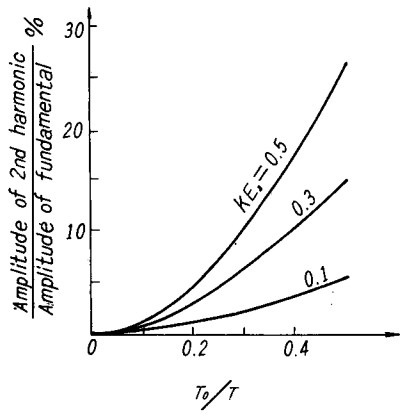

Fig. 11. Second harmonic of modulated pulse train.

The amplitude of the second harmonic is shown in Fig. 11 for $\tau_s/T_0=0.1$, where the ordinate shows the percentage of the harmonic to the fundamental. The third and the higher harmonics are much smaller and are negligible.

6. Motion of a Spool for Large Sinusoidal Input Signal

When the amplitude of the sinusoidal input is large, the input voltage exceeds the range of linear modulation, and finally the electric current cannot be switched in some part of the sinusoidal period. In this case the effect of saturation should be considered. However, if the sinusoidal input passes such an element as shown in Fig. 7 before it is given to the multivibrator, and the output of the saturation element is given to the multivibrator, the modulated

pulse train for large input is obtained, by using the modulation theory in the range of linear modulation formally. If the sinusoidal input, $E_a \sin \omega t$, passed the saturation element, the output $E(t)$ contains the odd harmonics as follows:

$$E(t) = E_1 \sin \omega t + E_3 \sin 3\omega t + E_5 \sin 5\omega t + \cdots \tag{17}$$

When the input signal of Eq. (17) is given to the multivibrator, the modulated pulse train is obtained as follows, corresponding to Eq. (12):

$$\begin{aligned}\frac{e(t)}{2y_m} &= \sum_{m=0}^{f_0 T_a - 1} \frac{1}{T_a}\left[\tau_0\{1+\kappa E_1 \sin \omega(m T_0 + t_0 - t_{D0}) + \kappa E_3 \sin 3\omega(m T_0 + t_0 - t_{D0}) + \cdots\} - \tau_s\right] \\ &+ \sum_{m=0}^{f_0 T_a - 1} \sum_{n=1}^{\infty} \frac{1}{(n\pi)^2} \frac{T_a}{\tau_s} \sin n\omega_a \tau_s \sin\left[\frac{n\omega_a \tau_0}{2}\{1+\kappa E_1 \sin \omega(m T_0 + t_0 - t_{D0})\right. \\ &\left. + \kappa E_3 \sin 3\omega(m T_0 + t_0 - t_{D0}) + \cdots\}\right] \cos n\omega_a (t - m T_0) \\ &- \sum_{m=0}^{f_0 T_a - 1} \sum_{n=1}^{\infty} \frac{1}{(n\pi)^2} \frac{T_a}{\tau_s} (1 - \cos n\omega_a \tau_s) \cos\left[\frac{n\omega_a \tau_0}{2}\{1+\kappa E_1 \sin \omega(m T_0 + t_0 - t_{D0})\right. \\ &\left. + \kappa E_3 \sin 3\omega(m T_0 + t_0 - t_{D0}) + \cdots\}\right] \cos n\omega_a (t - m T_0) . \end{aligned} \tag{18}$$

Eq. (18) is transformed as Eq. (13), and the equivalent transfer function $G_d(j\omega)$ is obtained as follows, considering the fundamental component:

$$\begin{aligned} G_d(j\omega) = \frac{y_m}{E_a} \frac{16}{(\omega T_0)^2} \frac{T_0}{\tau_s} \cos \frac{\omega T_0}{4} \sin \frac{\omega \tau_s}{2} J_1\left(\frac{k E_1 \omega T_0}{4}\right) \\ \times\left[J_0\left(\frac{k E_3 \omega T_0}{4}\right) J_0\left(\frac{k E_5 \omega T_0}{4}\right) \cdots\right] e^{-j\omega t_{D0}} , \end{aligned} \tag{19}$$

where J_1 and J_0 represent Bessel functions. When the spool displacement may be considered rectangular,

$$G_d(j\omega) = \frac{y_m}{E_a} \frac{8}{\omega T_0} \cos \frac{\omega T_0}{4} J_1\left(\frac{k E_1 \omega T_0}{4}\right)\left[J_0\left(\frac{k E_3 \omega T_0}{4}\right) J_0\left(\frac{k E_5 \omega T_0}{4}\right) \cdots\right] e^{-j\omega t_{D0}} . \tag{20}$$

From Eqs. (19) and (20), the gain of the equivalent transfer function is the function of E_1, E_3, E_5, etc., and the phase of the equivalent transfer function is determined only by the time lag of the spool movement. When the amplitude of higher harmonics is small, J_0 in Eq. (19) or (20) is approximately unity. Therefore, the output is approximately obtained by substituting E_1 in place of E_0 in J_1 of Eq. (14) or (16).

7. Frequency Characteristics of a Servo Loop

When mass and friction are considered as the load of the actuator, the characteristics of a spool valve are nonlinear, and its time constant depends on the input amplitude. Previously, the frequency characteristics were calculated by using Fourier series up to the third harmonics[3], and it was shown that the

flow characteristics shuld be approximated by the charateristics of a single-capacity-system, where the break point was chosen at the frequency of -3 db of the gain. The equivalent transfer function, $G(j\omega)$, of the combination of a spool valve and an actuator is represented as follows:

$$G(j\omega) = \frac{K_v}{j\omega(1+T_v j\omega)}, \tag{21}$$

where

$$K_v = \frac{C_q b\sqrt{p_s-(F_l/A_a)}}{A_a\sqrt{\rho}}, \qquad T_v = C_q b\sqrt{\frac{2}{\rho}}\,\frac{y_m M_l}{3A_a^2\sqrt{p_s-(F_l/A_a)}}. \tag{22}$$

The following nomenclatures are used in Eqs. (21) and (22): C_q=discharge coefficient of a valve port, b=width of a valve port, p_s=supply pressure, F_l=friction of a load, A_a=effective area of an actuator piston, M_l=mass of a load, ρ=density of oil.

As the amplitude of the dither is very small, and its period is short when compared to the sinusoidal input, the dither will not be fed back if the feedback path has a low pass characteristic a little. The feedback path may be considered to be a proportional element for sinusoidal frequencies, and its gain is represented by K_f.

The transfer function of the closed loop, $W(j\omega)$, is obtained as follows:

$$W(j\omega) = \frac{G_d(j\omega)G(j\omega)}{1+K_f G_d(j\omega)G(j\omega)}. \tag{23}$$

The maximum amplitude of the dither is the same as for no signals in spite of the modulation. The component corresponding to the pulse period in Eq. (13) represents the average amplitude of the dither during the period T_a.

8. Experiments

A two-stage electrohydraulic servo shown in Fig. 1 was manufactured for experiments. Principal dimensions are as follows:

diameter of a fixed orifice=1 mm,
diameter of a nozzle=2 mm,
displacement of a flapper=$\pm$0.17 mm,
displacement of a spool=$\pm$0.32 mm,
diameter of a spool=15 mm,
pulse repetition rate=87 cps,
b=2 mm, A_a=1.375 cm^2, p_s=40 kg/cm^2, M_l=0.0102 kg·s^2/cm,
F_l=6 kg, K_f=1.514 volt/cm, k=1.38 1/volt.

Using the above quantities, t_{D0} becomes 0·0027 s by calculations. The output displacement was detected by a differential transformer and recorded by an elec-

tromagnetic oscilloscope. The friction force of a load is given by the O-ring in the actuator. When the experimental apparatus is operated by an ordinary mode, a remarkable stick-slip motion occurs. However, when the PWM mode operation is applied to the same apparatus, the actuator piston moves smoothly even for very low velocity.

When the error voltage is below 0.25 volt, the modulation rate of pulses is proportional to the error voltage. The modulation is saturated when the error becomes 0.58 volt. The frequency characteristics of the open and closed loops are shown in Fig. 12 and Fig. 13, respectively. In these figures, the curves show the analytical results. When the input amplitude to the open loop is below

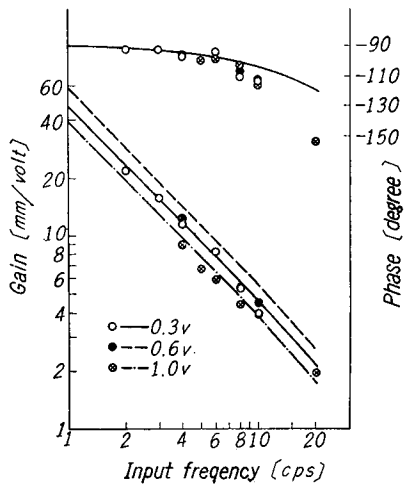

Fig. 12. Frequency characteristics of open loop.

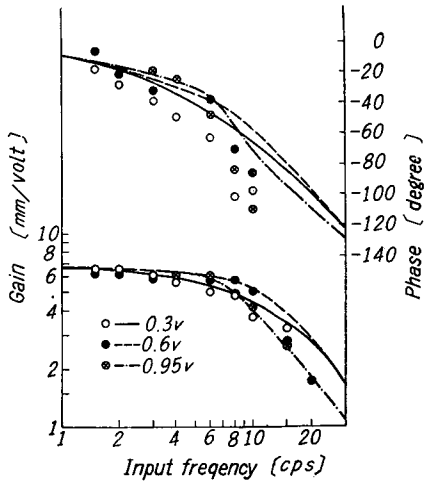

Fig. 13. Frequency characteristics of closed loop.

0.25 volt, the gain of the open loop is constant. When the input amplitude becomes large to some extent, the gain becomes higher. When it exceeds 0.6 volt, the saturation occurs and the equivalent gain becomes lower again. The phase lag of the open loop is determined chiefly by the integration characteristics at the actuator and the time lag of the spool motion.

In the closed loop, the gain becomes maximum when the error voltage is near 0.6 volt, and it decreases by the effect of saturation for larger error.

9. Conclusion

A two-stage electrohydraulic servo was manufactured for experiments, and the frequency characteristics were analyzed for the PWM mode operation. When the rectangular pulse current is given to two coils of the torquemotor

alternately, the spool is driven in the waveshape of trapezoidal pulse. The modulation of the pulse width is proportional to the input voltage for the small input signal. When the input voltage exceeds the range of linear modulation, the gain of modulation becomes higher, and finally the switching of the torque-motor circuit stops.

The trapezoidal pulse train modulated by the sinusoidal input was analyzed and the equivalent transfer function was obtained. When the input signal is large, the effect of saturation must be considered. In practice, the dither is effective when the actuator piston stops or moves at very low speed, while it is unnecessary when it moves at considerably high speed. Therefore, it is reasonable to design the PWM servo so that the modulation should be saturated by the input signal larger than a certain value.

Experimental results of frequency characteristics of the open loop and the closed loop were compared with calculated results for various signal frequencies and voltages.

Acknowledgement

The authors would like to express their appreciation to Prof. Y. SAWARAGI for his kind help in carring out this research.

References

1) J. E. Gibson and F. B. Tuteur; "Control System Components", McGraw-Hill, p. 389 (1958)
2) T. Sawamura, H. Hanafusa and T. Inui; J. Japan Association Automatic Control Engineers, **3**, 77 (1959)
3) T. Sawamura and H. Hanafusa; Proc. 8th JNCAM, p. 481 (1959)